Are There Equilibrium Intermediate States in the Urea-Induced Unfolding of Hen Egg-White Lysozyme?†

Beatriz Ibarra-Molero and Jose M. Sanchez-Ruiz*

Departamento de Quimica Fisica (Facultad de Ciencias) e Instituto de Biotecnologia, 18071-Granada, Spain

Received February 13, 1997; Revised Manuscript Received April 16, 1997⊗

ABSTRACT: Protein folding intermediates that are sometimes populated at equilibrium under mild denaturing conditions have attracted much attention as plausible models for the kinetic intermediates transiently populated in the refolding kinetic pathways. Hen egg-white lysozyme is often considered as a typical example of close adherence to the equilibrium, two-state unfolding mechanism. However, recent small-angle X-ray scattering studies suggest that an equilibrium intermediate state is significantly populated in the urea-induced unfolding of this protein at moderately acidic pH. In this work, we analyze the urea-induced unfolding of hen egg-white lysozyme on the basis of steady-state fluorescence measurements, characterization of the folding−unfolding kinetics, double-jump unfolding assays for the amount of native protein, and double-jump refolding assays for the amount of unfolded protein. Our results do not provide support for the presence of an intermediate state and, in particular, disfavor that the following two types of intermediates be significantly populated at equilibrium: (1) intermediates showing a substantial quenching of the tryptophan fluorescence (such as that observed in the transient intermediates found in the refolding kinetic pathway under strongly native conditions) and (2) associating intermediates. Also, the deconvolution of the radius of gyration unfolding profile by using the values for the amount of native state derived from our double-jump unfolding assays is consistent with a two-state unfolding equilibrium and suggests, furthermore, that, in this case, large alterations in the average structure of the unfolded ensemble do not take place in response to changes in urea concentration. This work points up possible pitfalls in the experimental detection of equilibrium folding intermediates and suggests procedures to circumvent them.

Under native conditions, the kinetics of protein folding *in vitro* is often complex, a fact usually ascribed to the heterogeneity of the unfolded state (likely due to proline isomerization; Brandts et al., 1975; Schmid, 1992) and to the presence of significantly populated intermediate states during the folding process (Kim & Baldwin, 1982, 1990). The transient nature of the kinetic intermediates renders difficult their characterization, which explains the current interest in the stable, equilibrium intermediates that are sometimes significantly populated at equilibrium under mild denaturing conditions and which might resemble the kinetic intermediates transiently populated in the kinetic refolding pathway [for recent reviews, see Dobson (1994), Ptitsyn (1995), Fink (1995), Freire (1995), and Privalov (1996)]. The careful small-angle X-ray scattering (SAXS)[1] studies recently reported by Chen et al. (1996) suggest the existence of an equilibrium intermediate in the urea-induced denaturation of hen egg white (HEW) lysozyme at pH 2.9. Chen et al. (1996) suggested that the structure of this equilibrium intermediate could correlate with that of the kinetic intermediate found in the refolding pathway of lysozyme under strongly native conditions (Radford et al., 1992). These are intriguing results, since HEW lysozyme is often considered a typical example of a model protein for which no significantly populated equilibrium intermediate states are observed. Thus, analysis of differential scanning calorimetry (DSC) thermograms for the thermal denaturation of this protein (Khechinashvili et al., 1973; Privalov & Khechinasvili, 1974; Pfeil & Privalov, 1976; Griko et al., 1995) indicates that no significant deviations from the equilibrium two-state unfolding mechanism occur. This result has been attributed (Griko et al., 1995) to the tight packing at the interface between the α and β domains, which, as a result, behave as a single cooperative unit in HEW lysozyme; by constrast, in the structurally homologous equine lysozyme the two domains unfold in two separate cooperative stages, possibly reflecting a looser packing at the interface between them (Griko et al., 1995). Also, no deviations from two-state mechanism were reported by Makhatadze and Privalov (1992) in their calorimetric study on the interactions of HEW lysozyme and other proteins with urea and guanidine [we note, however, that the DSC data reported by Makhatadze and Privalov (1992) span the 0−3 M denaturant concentration range, while, under the conditions employed by Chen et al. (1996), the urea-induced denaturation of HEW lysozyme occurs above 3 M urea]. On the other hand, Haezebrouck et al. (1995) provided evidence for the presence of a significantly populated (about 25%) equilibrium intermediate in the thermal denaturation of HEW lysozyme, but only at extreme pH conditions (pH 1.0), however. Finally, our recent analysis of the guanidine-induced denaturation of HEW lysozyme at pH 4.5 (Ibarra-Molero & Sanchez-Ruiz, 1996) indicates good adherence of the experimental data to the two-state mechanism with no equilibrium intermediate states.

In this work, we analyze the urea-induced unfolding of HEW lysozyme on the basis of the experimental approaches

† This research was supported by Grant PB93-1087 from the DGICYT (Spanish Ministry of Science and Education). B.I.-M. is a recipient of a predoctoral fellowship from the Spanish Ministry of Science and Education.

* To whom correspondence should be addressed. Fax: 34-58272879. E-mail: sanchezr@goliat.ugr.es.

⊗ Abstract published in *Advance ACS Abstracts,* July 1, 1997.

[1] Abbreviations: DSC, differential scanning calorimetry; HEW, hen egg white; SAXS, small-angle X-ray scattering; SVD, singular value decomposition.

S0006-2960(97)00330-9 CCC: $14.00

we employed in our recent study on the guanidine-induced denaturation of the protein (Ibarra-Molero & Sanchez-Ruiz, 1996): folding−unfolding kinetic measurements, equilibrium fluorescence measurements, and double-jump unfolding assays for the amount of native protein. In addition to these approaches, we explore in this work the possibility of determining the amount of unfolded state under given solvent conditions from the amplitude of the folding kinetics observed after transferring the protein to folding conditions. Mücke and Schmid (1994) realized the convenience of developing such *refolding assays*, but rightly pointed out that, unlike unfolding under denaturing conditions, the refolding of proteins is often a complex process involving parallel and sequential steps with different rates, a fact that would render very difficult the analysis of the refolding assays. As will be shown in this work, however, in the case of HEW lysozyme these complexities may be circumvented if the refolding assays are carried out under mild folding conditions.

The experimental data reported in this work do not provide support for the presence of a significantly populated intermediate state in the urea-induced unfolding of HEW lysozyme. This result will lead us to a reinterpretation of the small-angle X-ray scattering data in terms of the equilibrium, two-state unfolding mechanism (see Discussion). From a more general viewpoint, we believe that this work points up some possible pitfalls in the experimental detection of equilibrium folding intermediates and suggests procedures to circumvent them (see Concluding Remarks).

MATERIALS AND METHODS

Hen egg-white (HEW) lysozyme was purchased from Sigma Chemical Company, and guanidinium hydrochloride was ultrapure grade from Pierce. Both were used without further purification. Urea (SigmaUltra) was purchased from Sigma and purified by passage of its aqueous solutions through an AG 501-X8(D) ion exchange resine from Bio-Rad prior to adding the buffer components. Aqueous stock solutions of lysozyme were prepared by exhaustive dialysis against the desired buffer, usually sodium acetate 50 mM, pH 4.5 [the buffer conditions of Ibarra-Molero and Sanchez-Ruiz (1996)] or sodium citrate 100 mM, ClNa 100 mM, pH 2.9 [the buffer conditions of Chen et al. (1996)]. These two buffer conditions will be subsequently referred to as acetate buffer, pH 4.5 and citrate buffer, pH 2.9, respectively. Protein concentrations were determined spectrophotometrically, using a published value for the extintion coefficient at 280 nm (Canfield, 1963). Stock solutions of urea in the citrate buffer (usually at concentrations about 9 M) were prepared by mixing two solutions of urea in citric acid 100 mM with NaCl 100 mM and sodium citrate 100 mM with NaCl 100 mM, so that a pH meter reading of 2.9 was obtained (a small amount of HCl had to be added to the urea solution in citric acid in order to get a pH meter reading below 2.9); the buffer for the dialysis of the protein was prepared in the same manner, except that urea was not included. Lysozyme solutions in water−urea were prepared by mixing adequate amounts of the stock solution of urea, the aqueous stock solution of lysozyme and the dialysis buffer that had been equilibrated with the protein solution. The pH meter reading values for these lysozyme solutions in water−urea did not differ significantly (in less than 0.06 pH unit) from those of the stock solutions. Lysozyme solutions in water−guanidine (sodium acetate buffer, pH 4.5) were prepared as described by Ibarra-Molero and Sanchez-Ruiz (1996). Guanidine and urea concentrations were determined from refraction index measurements (Pace et al., 1989). Protein fluorescence in urea and guanidine solutions was measured by using a Perkin-Elmer LS-5 instrument with excitation and emission wavelengths of 280 and 360 nm, respectively, with a protein concentration around 3 μM. All measurements were carried out at 20 °C.

Double-Jump Unfolding Assays. Unfolding assays were carried out as described by Ibarra-Molero and Sanchez-Ruiz (1996). Briefly, protein (at concentrations of 7 or 10 mg/mL) was incubated in urea solutions (the "initial" solutions) at 20 °C for a time sufficient to ensure that the unfolding equilibrium had been established, and subsequently, the unfolding kinetics were initiated by dilution into high guanidine (7.3−8.1 M), sodium acetate 50 mM, pH 4.5 (under these conditions, the relaxation time for native state denaturation is of the order of a few minutes); 155-fold and 220-fold dilutions were carried out for protein concentrations in the urea solutions of 7 and 10 mg/mL, respectively. Unfolding kinetics were monitored by following the time dependence of the fluorescence emission at 360 nm. Fluorescence intensity versus time profiles gave excellent fits to the following first-order rate equation:

$$I = I_\infty - \Delta I e^{-t/\tau} \qquad (1)$$

where I_∞ is the fluorescence intensity at $t = \infty$ and ΔI stands for the amplitude of the exponential, which is proportional to the mole fraction of native state in the original urea solution: $\Delta I = \Delta I^0 X_N$. In fact, the program MLAB (Civilized software, Inc.) was used to perform the global fitting of eq 1 to each series of several unfolding kinetics carried out under the same unfolding assay conditions and corresponding to the same protein concentration in the initial urea solutions. In this kind of global fitting, we impose that the value of the denaturation relaxation time (τ in eq 1) under the unfolding assay conditions must be the same for all kinetic profiles, while we allow each kinetic profile to have its own I_∞ and ΔI values.

Double-Jump Refolding Assays. Refolding assays were carried out and analyzed essentially as described above for the unfolding assays but, in this case, the second jump was a dilution to *mild* folding conditions: 3.2 M guanidine in acetate buffer, pH 4.5. We have found that, under these conditions, the refolding of protein previously incubated in denaturing concentrations of urea or guanidine can be described by a single exponential (refolding relaxation time of a few minutes). This simple result was to be expected because (1) kinetic intermediate states in the refolding of HEW lysozyme only appear to become significantly populated at guanidine concentrations significantly lower than 3.2 M [see, for instance, the Chevron plot of Figure 3 in Kiefhaber (1995)] and (2) in the case of HEW lysozyme, little kinetic complexity seems to arise from heterogeneity in the unfolded state; thus, under native conditions, only 10% of the molecules appear to refold through a slow phase, believed to result from proline isomerization (Kato et al., 1981). Furthermore, we have never detected such slow-phase in our refolding experiments under mild folding conditions, possibly because the equilibrium between the fast-folding and slow-folding species is established in the time scale of our refolding experiments and, therefore, the fast-

folding and slow-folding molecules behave as a single species from a kinetic point of view.

Refolding kinetics were monitored by following the time dependence of the fluorescence intensity at 360 nm and were fitted with the following equation:

$$I = I_\infty + \Delta I e^{-t/\tau} \quad (2)$$

In fact, global analyses, similar to those described for the unfolding assays were carried out using the program MLAB.

Folding−Unfolding Kinetics. Folding−unfolding kinetics were studied by following the time dependence of the protein fluorescence emission at 360 nm after suitable denaturant concentration jumps in a manner similar to that described by Ibarra-Molero and Sanchez-Ruiz (1996). Apparent folding−unfolding rate constants (k) were calculated from the fittings of a first-order rate equation ($I = I_\infty - \Delta I e^{-kt}$) to the experimental fluorescence intensity versus time profiles. These fits were excellent.

In addition, interrupted unfolding experiments were used to characterize the folding−unfolding kinetics at urea concentrations within the transition zone. These experiments are simply a kinetic version of the double-jump unfolding assays. Briefly, native protein was transferred to the urea solutions, after a variable delay time diluted into 7.5 M guanidine, acetate buffer, pH 4.5, and the mole fractions of native protein were calculated from the fluorescence-detected unfolding kinetics.

RESULTS

Urea-Induced Unfolding of HEW Lysozyme in Citrate Buffer, pH 2.9, as Monitored by Double-Jump Unfolding Assays. For a protein concentration in the initial urea solutions of 7 mg/mL, we performed 13 double-jump unfolding experiments at 20 °C spanning a wide range of urea concentration that included the transition zone. Figure 1A shows some examples of the obtained fluorescence-detected unfolding kinetics. A good global fit of the first-order rate equation (eq 1) to the 13 unfolding profiles was obtained imposing a common value for the unfolding relaxation time (Figure 1A). The effect of urea concentration (C) in the initial solution on the calculated amplitude of the unfolding kinetics (ΔI) is shown in Figure 1B. This ΔI versus C profile was analyzed according to the following equation:

$$\Delta I = \frac{\Delta I^0}{1 + e^{m_{1/2}(C - C_{1/2})/RT}} \quad (3)$$

where $C_{1/2}$ is the denaturant concentration at which the denaturation Gibbs energy is zero and $m_{1/2}$ is the minus derivative ($\partial\Delta G/\partial C$) at $C_{1/2}$. The values obtained for $C_{1/2}$ and $m_{1/2}$ are given in Table 1. Equation 3 does not involve the linear extrapolation approximation,[2] although it does assume a two-state denaturation mechanism. Note, nevertheless, that the main purpose of the fitting of eq 3 to the ΔI versus C profiles is the reliable determination of ΔI^0 (which equals the value of ΔI at denaturant concentrations clearly below the transition zone, see Figure 1B). In fact, the calculation of the mole fraction of protein present as native state from $X_N = \Delta I/\Delta I^0$ does not involve the two-state assumption (Mücke & Schmid, 1994). The values of X_N thus calculated are plotted versus urea concentration in Figure 2.

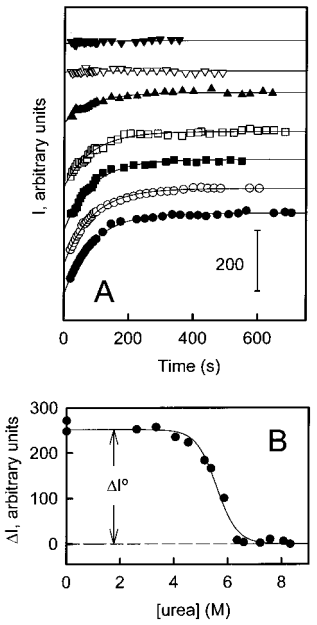

FIGURE 1: (A) Examples of the profiles of fluorescence intensity versus time recorded after transferring HEW lysozyme, previously incubated in a given urea solution (citrate buffer, pH 2.9) until equilibrium had been established, to strongly denaturing conditions (8.1 M guanidine, acetate buffer, pH 4.5). The urea concentrations in the initial solutions are (●) 0 M, (○) 2.6 M, (■) 4.0 M, (□) 5.1 M, (▲) 5.8 M, (▽) 6.6 M, (▼) 7.6 M. The protein concentration in the initial solution was 7 mg/mL in all cases. The lines represent the best global fit of eq 1 to all the kinetic unfolding profiles; in this kind of fitting, we impose that the value of the unfolding relaxation time must be the same for all kinetic profiles. (B) Unfolding amplitudes calculated from the global fitting of eq 1 to the unfolding kinetics. These amplitudes are proportional to the amount of native protein in the initial solutions and are plotted versus the urea concentration in those solutions. The line represents the best fit of eq 3 to the unfolding amplitude data.

Table 1: Values of $C_{1/2}$ and $m_{1/2}$ for the Urea-Induced Unfolding of HEW Lysozyme at pH 2.9

approach	protein concentration (mg/mL)	$C_{1/2}$ (M)	$m_{1/2}$ (kJ mol^{-1} M^{-1})
unfolding assays	7	5.58 ± 0.04	6.7 ± 0.7
unfolding assays	10	5.69 ± 0.14	*a*
refolding assays	7	5.51 ± 0.07	5.3 ± 0.8
refolding assays	10	5.53 ± 0.04	*a*
Chevron plot	0.046	5.75 ± 0.23	6.0 ± 0.5
fluorescence with linear unfolded baseline	0.046	5.69 ± 0.06	5.6 ± 0.8
fluorescence with nonlinear unfolded baseline	0.046	5.63 ± 0.06	6.3 ± 1.0
global analysis of radius of gyration and circular dichroism data	*b*	5.51 ± 0.06	5.3 ± 0.4

[a] A reliable estimate of $m_{1/2}$ cannot be obtained in this case since only three experiments were carried out. [b] See Chen et al. (1996) for the several concentrations employed.

[2] Equilibrium unfolding profiles are not sensitive to the details of the denaturant concentration dependence of the unfolding ΔG outside the narrow transition region. Two-state equations employed in this work (eq 3 is an example) do not involve the linear extrapolation approximation, since they assume a linear dependence of ΔG [$\Delta G = -m_{1/2}(C - C_{1/2})$] only within the transition region [see Ibarra-Molero and Sanchez-Ruiz (1996) and Schellman (1987)]. The linear extrapolation approximation would only be invoked if ΔG at zero denaturant concentration is calculated from the transition parameters by using $\Delta G_W = m_{1/2}C_{1/2}$.

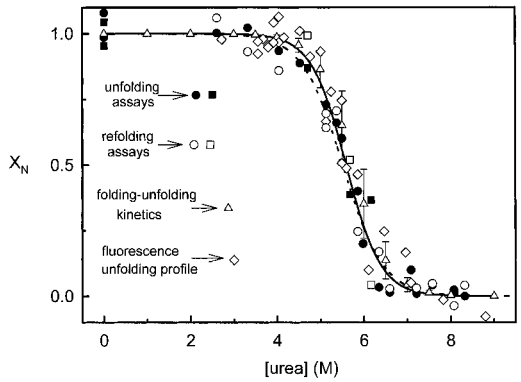

FIGURE 2: Equilibrium profile of mole fraction of native protein versus urea concentration for HEW lysozyme in citrate buffer, pH 2.9. (●) Values calculated from the unfolding assays carried out with a protein concentration in the initial solutions of 7 mg/mL, (■) values calculated from the unfolding assays carried out with a protein concentration in the initial solutions of 10 mg/mL, (○) values calculated (as $1 - X_U$) from the refolding assays (Figure 3) carried out with a protein concentration in the initial solutions of 7 mg/mL, (□) values calculated (as $1 - X_U$) from the refolding assays carried out with a protein concentration in the initial solutions of 10 mg/mL, (◇) values calculated from the fluorescence unfolding profile (Figure 5) by using $X_N = (I_U - I)/(I_U - I_N)$ where the values of I_N and I_U are given by the linear baselines (the use of the quadratic baseline for I_U yields essentially the same results), (△) values calculated from the $m_{1/2}$ and $C_{1/2}$ data (Table 1) derived from the analysis (eq 6) of the Chevron plot in Figure 4A (the bars stand for the associated standard errors, as estimated from those of $m_{1/2}$ and $C_{1/2}$). The continuous line is that predicted by the (weighted) averages of the $m_{1/2}$ and $C_{1/2}$ values derived from the several experimental approaches employed in this work. The dashed line is calculated from the $m_{1/2}$ and $C_{1/2}$ values obtained from the global analysis (Figure 7) of the data of Chen et al. (1996). All the calculations of X_N from $C_{1/2}$ and $m_{1/2}$ data employ the two following equations: $\Delta G = -m_{1/2}(C - C_{1/2})$ and $X_N = [1 + \exp(-\Delta G/RT)]^{-1}$.

For protein concentrations in the original urea solutions of 10 mg/mL, we only carried out three double-jump unfolding assays, spanning a limited urea concentration range within the transition zone. In these cases, the values of ΔI^0 required for the calculation of X_N were derived from control assays in which the second jump was performed from strongly native conditions (aqueous citrate buffer, pH 2.9). Again, the values obtained for X_N are given in Figure 2.

Urea-Induced Unfolding of HEW Lysozyme in Citrate Buffer, pH 2.9, as Monitored by Double-Jump Refolding Assays. Thirteen double-jump refolding experiments were carried out with a protein concentration in the initial urea solutions of 7 mg/mL. A good global fit of the first-order rate equation (eq 2) to the 13 refolding profiles were obtained imposing a common value for the refolding relaxation time (Figure 3A). The resulting ΔI (amplitude of the refolding kinetics) versus urea concentration profile was analyzed according to the following two-state equation:

$$\Delta I = \frac{\Delta I^0 e^{m_{1/2}(C - C_{1/2})/RT}}{1 + e^{m_{1/2}(C - C_{1/2})/RT}} \quad (4)$$

The values obtained for $C_{1/2}$ and $m_{1/2}$ are given in Table 1. The main purpose of the fitting of eq 4 to the $\Delta I/C$ data was to determine ΔI^0, the refolding amplitude corresponding to 100% unfolded protein, which equals the ΔI value at denaturant concentrations clearly above the transition zone

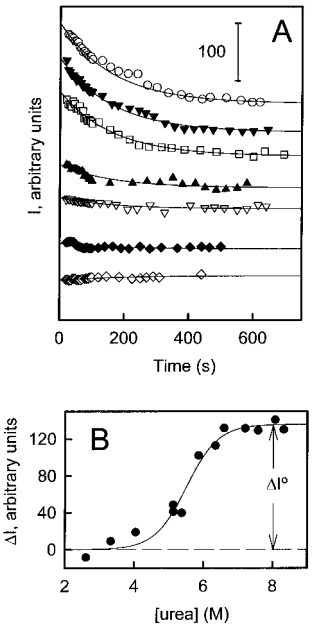

FIGURE 3: (A) Examples of the profiles of fluorescence intensity versus time recorded after transferring HEW lysozyme, previously incubated in a given urea solution (citrate buffer, pH 2.9) until equilibrium had been established, to mild folding conditions (3.2 M guanidine, acetate buffer, pH 4.5). The urea concentrations in the initial solutions are (▼) 7.6 M, (□) 6.3 M, (▲) 5.4 M, (▽) 4.0 M, (◆) 3.3 M, (◇) 2.6 M. The data represented by ○ correspond to a control experiment in which the protein had been incubated in a high guanidine solution (7.5 M) in acetate buffer, pH 4.5. The protein concentration in the initial solutions was 7 mg/mL in all cases. The lines represent the best global fit of eq 2 to all the kinetic unfolding profiles; in this kind of fitting, we impose that the value of the refolding relaxation time must be the same for all kinetic profiles. (B) Refolding amplitudes calculated from the global fitting of eq 2 to the refolding kinetics. These amplitudes are plotted versus the urea concentration in the initial solutions. The line represents the best fit of eq 4 to the refolding amplitude data.

(see Figure 3B). The mole fraction of protein present as unfolded state in the initial urea solutions may be then calculated as $X_U = \Delta I/\Delta I^0$ (of course, the mole fraction of "unfolded" protein thus calculated might, perhaps, include the amount of intermediate states in fast equilibrium with the "true" unfolded state under the conditions of the refolding assay, see Discussion). For the sake of comparison, in Figure 2 we have actually plotted the values of the fraction of native protein calculated as $X_N = 1 - X_U$.

Three double-jump refolding assay experiments were carried with protein concentrations in the initial urea solutions of 10 mg/mL (the same solutions employed in the unfolding assays previously described). In these cases, the values of ΔI^0 required for the calculation of X_U were derived from control assays in which the second jump was performed from a strongly denaturing solution (8 M guanidine in acetate buffer, pH 4.5). In Figure 2 we give, in fact, X_N values calculated as $1 - X_U$.

Urea-Dependence of the Folding−Unfolding Kinetics of HEW Lysozyme in Citrate Buffer, pH 2.9. Apparent, folding−unfolding rate constants (k) in the presence of urea were obtained from fluorescence-detected kinetics after suitable denaturant concentration jumps (Figure 4A). In addition, interrupted unfolding experiments were used to characterize the folding−unfolding kinetics at four urea concentrations within the transition zone; the corresponding profiles of X_N versus time (Figure 4B) gave good fits to the

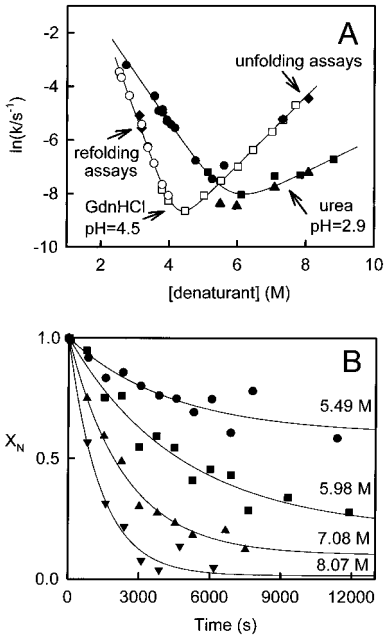

FIGURE 4: (A) Chevron plots of folding−unfolding rate constant for HEW lysozyme versus denaturant (urea or guanidine) concentration. The lines are the best fits of eq 6 to the data.The meaning of the symbols is as follows. Guanidine-induced unfolding, acetate buffer, pH 4.5: (□) experiments carried out in the unfolding direction, (○) experiments carried out in the folding direction, (◆) values obtained from the analysis of the double-jump unfolding and refolding experiments (see Figures 1 and 3). Urea-induced unfolding, citrate buffer, pH 2.9: (■) experiments carried out in the unfolding direction, (●) experiments carried out in the folding direction, (▲) values calculated from the interrupted unfolding experiments shown in panel B. (B) The kinetics of the urea-induced unfolding of HEW lysozyme in citrate buffer, pH 2.9, as monitored by interrupted unfolding experiments. The mole fractions of native protein (X_N) given in this figure have been determined from unfolding assays (see Materials and Methods for details). The lines are the best fits of eq 5 to the data. The numbers alongside the lines stand for the urea concentration.

following first-order rate equation:

$$X_N(t) = X_{N,\infty} + (1 - X_{N,\infty})e^{-kt} \quad (5)$$

where $X_{N,\infty}$ is the mole fraction of native protein at equilibrium. The values of k calculated from these fittings were in acceptable agreement with those derived from the fluorescence intensity versus time profiles (Figure 4A). For the sake of comparison, we also include in Figure 4A the guanidine dependence of the folding−unfolding kinetics in acetate buffer, pH 4.5.

The denaturant concentration dependence of the folding−unfolding rate constants (see the Chevron plot of Figure 4A) was analyzed according to a two-state *kinetic* model ($k = k_F + k_U$):

$$\ln k = \ln k_{1/2} + \ln\left[\exp\left(\frac{m_{U-\ddagger}}{RT}(C - C_{1/2})\right) + \exp\left(\frac{m_{N-\ddagger}}{RT}(C - C_{1/2})\right)\right] \quad (6)$$

where $m_{U-\ddagger}$ and $m_{N-\ddagger}$ describe the denaturant concentration dependence of the activation Gibbs energies for folding and unfolding, respectively [$m_{U-\ddagger} = -(\partial\Delta G_F/\partial C)$, $m_{N-\ddagger} = -(\partial\Delta G_U/\partial C)$], and $k_{1/2}$ is the value of both the folding (k_F) and unfolding (k_U) rate constants at $C = C_{1/2}$. Equation 6 assumes that $m_{U-\ddagger}$ and $m_{N-\ddagger}$ may be taken as constants within the studied denaturant concentration range and can be easily derived from transition state theory (Chen et al., 1992; Ibarra-Molero & Sanchez-Ruiz, 1996). A good fit of eq 6 to the ln k versus C profile was obtained (see Figure 4A); the fitting parameters were $C_{1/2}$, $k_{1/2}$, $m_{U-\ddagger}$, and $m_{N-\ddagger}$ but the equilibrium $m_{1/2}$ value could be calculated from the kinetic m values as $m_{N-\ddagger} - m_{U-\ddagger}$. The values obtained for $C_{1/2}$ and $m_{1/2}$ are given in Table 1. The profile of X_N versus urea concentration predicted by these $C_{1/2}$ and $m_{1/2}$ values is shown in Figure 2.

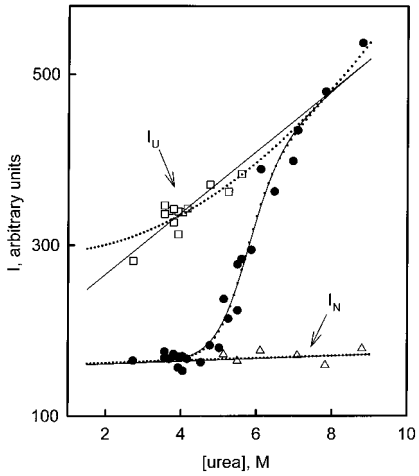

FIGURE 5: The urea-induced equilibrium unfolding of HEW lysozyme in citrate buffer, pH 2.9, as monitored by fluorescence emission. Three data sets are included in this figure: (●) fluorescence intensity values measured at equilibrium, (□) intensity values for the unfolded state calculated as the zero-time extrapolations of the fluorescence-detected refolding kinetic profiles recorded after denaturant concentration jumps from strongly unfolding conditions (8 M urea, citrate buffer, pH 2.9), (△) intensity values for the native state calculated as the zero-time extrapolations of the fluorescence-detected unfolding profiles recorded after denaturant concentration jumps from native conditions (citrate buffer, pH 2.9, in the absence of urea). In all cases (●, □, and △) the protein concentration is 0.046 mg/mL. The continuous lines represent the best simultaneous fit of eq 7 and linear equations for the unfolded and native fluorescence baselines, to the experimental I, I_U, and I_N data, respectively. The results of the same global fit, but assuming a quadratic unfolded baseline, is shown with dotted lines.

Equilibrium Fluorescence Profile for the Urea-Induced Unfolding of Lysozyme. Figure 5 shows an equilibrium profile of fluorescence intensity at 360 nm versus urea concentration (citrate buffer, pH 2.9). This profile was analyzed on the basis of the following two-state equation:

$$I = \frac{I_N + I_U e^{m_{1/2}(C - C_{1/2})/RT}}{1 + e^{m_{1/2}(C - C_{1/2})/RT}} \quad (7)$$

where I_N and I_U are the fluorescence intensities for the native and unfolded states (that is, the fluorescence baselines). In order to minimize the uncertainties associated with baseline determination, we have included in the analysis the I_N and I_U values given by the zero-time extrapolations of fluorescence-detected unfolding and folding kinetic profiles. Note that, since the I_N and I_U values calculated in this way span a wide concentration range (see Figure 5), the possible nonlinearity of their denaturant concentration dependence may be taken into account in the analysis; see legend to Figure 5 for further details. The values of $m_{1/2}$ and $C_{1/2}$ derived from the analysis of the fluorescence data in Figure 5 are given in Table 1 and the corresponding X_N versus C profile is shown in Figure 2.

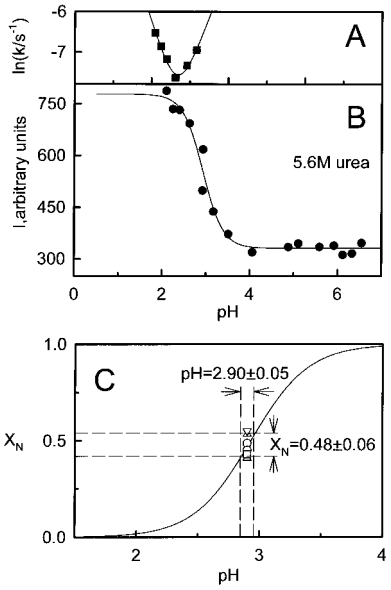

FIGURE 6: The pH-induced unfolding of HEW lysozyme at an urea concentration of 5.6 M. (A) Rate constants obtained from the first-order analysis of fluorescence-detected unfolding kinetic profiles recorded after denaturant concentration jumps from native conditions (citrate buffer, pH 2.9 in the absence of urea) to 5.6 M urea and different pHs in citrate buffer. The line represents the best fit of eq 10 to the data. (B) Equilibrium fluorescence intensity versus pH profile. The line represents the best fit of eq 8 to the data. (C) Profile of mole fraction of native protein versus pH corresponding to the transition shown in panel B. The symbols represent the X_N values at 5.6 M and pH 2.9 calculated by using the $C_{1/2}$ and $m_{1/2}$ values given in Table 1: (○) folding and unfolding assays at 7 mg/mL, (△) folding and unfolding assays at 10 mg/mL, (□) chevron plot, (▽) equilibrium fluorescence data. These values yield an average X_N of 0.48 with a standard deviation of 0.06. The figure illustrates the fact that the observed scatter in the X_N values could be explained by a scatter in the pH value of only ±0.05.

pH-Induced Unfolding of HEW Lysozyme at Denaturing Urea Concentrations. We have studied the effect of pH on the protein fluorescence emission in sodium citrate buffer 100 mM with NaCl 100 mM and a urea concentration of 5.6 M. The fluorescence intensity versus pH profile shows a sharp transition due to the pH-induced unfolding of the protein (Figure 6). This profile was analyzed according to the following two-state equation

$$I = \frac{I_N + I_U e^{-(\ln 10)\Delta\nu(pH - pH_{1/2})}}{1 + e^{-(\ln 10)\Delta\nu(pH - pH_{1/2})}} \quad (8)$$

where $\Delta\nu$ is the number of protons taken by the protein from the solvent upon unfolding and $pH_{1/2}$ is the pH value at which the unfolding Gibbs energy (ΔG) is zero (we expect $pH_{1/2} \approx 2.9$, since 5.6 M $\approx C_{1/2}$ for pH 2.9; Table 1). Equation 8 can be easily derived from that giving the pH effect on ΔG (Alberty, 1969; Plaza del Pino & Sanchez-Ruiz, 1995):

$$\left(\frac{\partial \Delta G}{\partial pH}\right)_{T,[urea]} = (\ln 10)RT\Delta\nu \quad (9)$$

by assuming that $\Delta\nu$ may be taken as a constant within the narrow range of the pH-induced transition. The nonlinear, least-squares fitting of eq 8 to the experimental I versus pH profile assuming pH-independent I_N and I_U values (see Figure 6B) yields a $\Delta\nu$ value of 1.9 ± 0.4 mol of H^+/mol of protein.

We also include in Figure 6 some experimental data on the effect of pH on the folding−unfolding rate constant (with k values obtained from the analysis of fluorescence-detected unfolding kinetics as previously described). These data were analyzed according to the following two-state equation:

$$\ln k = \ln k_{1/2} + \ln[\exp(-(\ln 10)\Delta\nu_{N-\ddagger}(pH - pH_{1/2})) + \exp(-(\ln 10)\Delta\nu_{U-\ddagger}(pH - pH_{1/2}))] \quad (10)$$

where $k_{1/2}$ is the value of both the folding and unfolding rate constants at $pH_{1/2}$ and $\Delta\nu_{N-\ddagger}$ and $\Delta\nu_{U-\ddagger}$ are the differences between the number of protons bound to the transition state and the native and unfolded states, respectively. Equation 10 is easily derived from transition state theory and assumes $\Delta\nu_{N-\ddagger}$ and $\Delta\nu_{U-\ddagger}$ may be taken as constants within the narrow range of the pH-induced transition. The number of protons taken by the protein from the solvent upon unfolding may be computed from the kinetic values by using: $\Delta\nu = \Delta\nu_{N-\ddagger} - \Delta\nu_{U-\ddagger}$. From the fitting of eq 10 to the experimental ln k/pH data, we calculate $\Delta\nu = 2.4 \pm 0.5$ (see Figure 6A). The values we have obtained for $\Delta\nu$ at pH 2.9 and 5.6 M urea (1.9 ± 0.4 and 2.4 ± 0.5) are similar, but somewhat smaller, than those given by Pfeil and Privalov (1976) in the absence of urea (around 3.3 for pH 2.9).

The sharpness of the pH-induced transition at denaturating urea concentrations has an important consequence: very small pH changes may cause measurable changes in the relative amounts of the native and unfolded states and, we note, under the normal laboratory practice, pH values cannot usually be measured and reproduced with a precission better than a few hundreths of a pH unit.[3] Clearly, this "pH-irreproducibility" effect may be a significant source of discrepancy between experimental unfolding profiles. A pictorial illustration of this effect is given in Figure 6C.

DISCUSSION

Experimental Data Reported in this Work Do Not Provide Support for the Presence of a Significantly Populated Intermediate State in the Urea-Induced Unfolding of HEW Lysozyme. The results obtained in this work are summarized in Figure 2 as profiles of mole fraction of native protein (X_N) versus urea concentration for HEW lysozyme unfolding in sodium citrate 100 mM, NaCl 100 mM, pH 2.9 (the values of $C_{1/2}$ and $m_{1/2}$ corresponding to these profiles are collected in Table 1). The data in this figure have been calculated from four different approaches: (A) double-jump unfolding assays; (B) double-jump refolding assays; (C) analysis of the urea dependence of the apparent folding−unfolding rate constants; and (D) analysis of the equilibrium fluorescence profile for urea-induced denaturation. We note that methods C and D for the calculation of X_N assume a two-state mechanism, while methods A and B do not. We also note that baseline problems do not arise with methods A−C and that they have been minimized in method D by including in the analysis the fluorescence intensity values for the native and unfolded states given by the zero-time extrapolations of the fluorescence-detected unfolding and folding kinetics (Figure 5).

[3] In principle, with well-buffered aqueous solutions, pH measurements can be reproduced to about 0.02 pH unit. This, however, requires a very careful operational procedure [see, for instance, pages 422−424 in Bates (1973)]. It is safe to assume that a larger irreproducibility is associated to pH measurements under the normal laboratory practice.

As shown in Figure 2, there is a good agreement between the X_N values derived from the four experimental approaches described above. We must note, nevertheless, that the presence of intermediates might not be apparent in folding−unfolding kinetics and double-jump refolding assays if the intermediates are always in fast equilibrium with the unfolded state in the time scales of the kinetic experiments (Mücke & Schmid, 1994). This obvious caveat notwithstanding, it is clear that our results do not provide support for the presence of an intermediate state in the urea-induced unfolding of HEW lysozyme at pH 2.9 and, in particular, they do disfavor that the following two types of intermediates be significantly populated at equilibrium in this case:

(1) Intermediates similar to those found in the refolding pathway of HEW lysozyme under strongly native conditions (Radford et al., 1992); it appears now that these intermediates are characterized by non-native interactions of tryptophan residues (Denton et al., 1994; Rothwarf & Scheraga, 1996) which are reflected in a very strong quenching of the tryptophan fluorescence in such a way that their fluorescence emission intensity at 360 nm is much lower than that of both, the native and unfolded states (Denton et al., 1994; Itzhaki et al., 1994; Kiefhaber, 1995; Itzhaki & Evans, 1996; Rothwarf & Scheraga, 1996; Lu et al., 1997). Therefore, the presence of this type of intermediate would have been glaringly evident in our fluorescence-detected kinetic and equilibrium experiments.

(2) Associating intermediate states; recent work supports that equilibrium intermediate states in the thermal or solvent-induced unfolding of proteins may show a strong tendency to associate (Filimonov & Rogov, 1996; Semitsonov et al., 1996). Associated intermediates, however, are unlikely to be significantly populated in the urea-induced unfolding of HEW lysozyme at pH 2.9, since their presence would have caused a protein concentration dependence of the denaturation profiles; this dependence would have been easily revealed by our data, which span a 200-fold change in protein concentration. However, no significant protein concentration effect on the denaturation profiles was found (Figure 2 and Table 1).

Reinterpretation of the Small-Angle X-ray Scattering Data in Terms of the Equilibrium, Two-State Mechanism. The careful small-angle X-ray scattering study recently reported by Chen et al. (1996) suggests a two-fold evidence for the existence of a significantly populated equilibrium intermediate in the urea-induced unfolding of HEW lysozyme at pH 2.9: (1) differences in the unfolding profiles monitored by the radius of gyration and by far-UV and near-UV circular dichroism; (2) the presence of a third basis component in the Singular Value Decomposition (SVD) analysis of the urea dependence of the X-ray scattering curves.

However, a minor discrepancy [such as that reported by Chen et al. (1996)] between the unfolding profiles monitored by different physical probes may be an apparent effect due to baseline tracing. In order to show this point, we have carried out a global fitting of the following two-state equation to the three unfolding profiles reported by Chen et al. (the urea dependencies of the squared radius of gyration, the ellipticity at 222 nm and the ellipticity at 289 nm):

$$P = \frac{P_N + P_U e^{m_{1/2}(C - C_{1/2})/RT}}{1 + e^{m_{1/2}(C - C_{1/2})/RT}} \qquad (11)$$

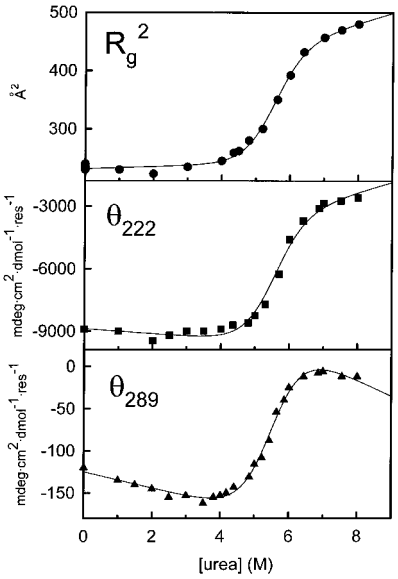

FIGURE 7: Global analysis of the urea-induced unfolding profiles for HEW lysozyme at pH 2.9 as monitored by the squared radius of gyration, the ellipticity at 222 nm and the ellipticity at 289 nm [data taken from Chen et al. (1996)]. The lines represent the best global fit of eq 11 to the data, imposing that the values of $m_{1/2}$ and $C_{1/2}$ must be the same for the three profiles; on the other hand, the native and unfolded baselines (taken as linear functions of the urea concentration) were independently fitted for each profile. The global analysis weighted the data according to the inverse of the variance in each profile. The required variances were roughly estimated from the residuals of the fit of a straight line to the data in the 0−3 M urea concentration range. The reduced χ^2 value for the global fit was 2.1.

where P is R_g^2, θ_{222}, or θ_{289}. The global fit of eq 11 was carried out imposing that the values of $m_{1/2}$ and $C_{1/2}$ must be the same for the three profiles, while each profile was allowed to have its own native and unfolded baselines (P_N and P_U, respectively). A good global fit was obtained by taking the baselines as linear functions of urea concentration (see Figure 7 and its legend for details). This result supports that the three experimental profiles are consistent with the same two-state unfolding transition in terms of mole fraction of native protein versus urea concentration, since only the common parameters ($m_{1/2}$ and $C_{1/2}$) determine the value of X_N. Also, this unfolding transition is in excellent agreement with that derived from the experimental results reported in this work (see Table 1 and Figure 2).

Clearly, the discrepancy reported by Chen et al. (1996) between the R_g^2, θ_{222}, and θ_{289} unfolding profiles could be explained in terms of a baseline effect alone (Figure 7) and, in addition, we cannot rule out that some contribution to the apparent discrepancy arises from the "pH-irreproducibility" effect previously pointed out (see Figure 6 and Concluding Remarks). We conclude, therefore, that these R_g^2, θ_{222}, and θ_{289} unfolding profiles do not provide reliable evidence for the presence of a significantly populated equilibrium intermediate in the urea-induced unfolding of HEW lysozyme at pH 2.9. Also, it is not clear that reliable evidence is provided by the SVD analysis of the X-ray scattering profiles. Thus, the coefficient (b_3) of the third basis function in the SVD analysis is not well-defined [see Figure 6 in Chen et al. (1996)], and conceivably, the third basis component might be compensating for some noise-like effect (perhaps associated with a small scatter in the pH values of the several urea solutions?). Chen et al. were obviously aware of this

problem and, in connection with the SVD analysis, they stated that "the fits for b_1 and b_2 were reasonable, where as the result for b_3 was clearly less well defined. Again, the quality of scattering data available at the present time may not be adequate for a reliable interpretation of the lysozyme unfolding mechanism taken on their own, but, by considering them along with the analysis of the denaturation curves, the reliability of the fits is considerably increased". However, we have shown that the denaturation curves (the unfolding profiles of Figure 7 in this work) may be reasonably explained in terms of a two-state unfolding mechanism; it appears, therefore, that the three-states interpretation of the SVD analysis has been deprived of its main support.

As an alternative to the intermediate state picture, we could consider the possibility [as Chen et al. (1996) did, in fact] that the SAXS data for the urea-induced unfolding of HEW lysozyme reflected a gradual alteration in the "average structure" of the unfolded ensemble. In order to test this possibility, we have removed the contribution of the native state to the radius of gyration data of Chen et al. (1996) and calculated the average of the squared radius of gyration over all the protein states *but excluding the native one*:

$$\langle R_g^2 \rangle_U = \frac{R_g^2 - X_N R_{g,N}^2}{1 - X_N} \qquad (12)$$

where R_g^2 is the squared radius of gyration at a given denaturant concentration, X_N is the mole fraction of native protein at that denaturant concentration, and $R_{g,N}^2$ is the squared radius of gyration for the native state. The values thus calculated may be interpreted [see Smith et al. (1996)] as the apparent radius of gyration of the unfolded state (hence the subindex U we have used in eq 12). The results of the calculation (eq 12) for the urea-induced unfolding of HEW lysozyme at pH 2.9 are shown in Figure 8. Clearly, the apparent radius of gyration for the unfolded state changes comparatively little with urea concentration, which suggests that, in this case, large alterations in the average structure of the unfolded ensemble do not occur in reponse to changes in urea concentration [compare with the results reported by Smith et al. (1996) on mutants of the β1variant of the B1 domain of streptococcal Protein G]. Note also that the analysis given in Figure 8 supports that the radius of gyration unfolding profile may be interpreted in terms of a two-state equilibrium mechanism.

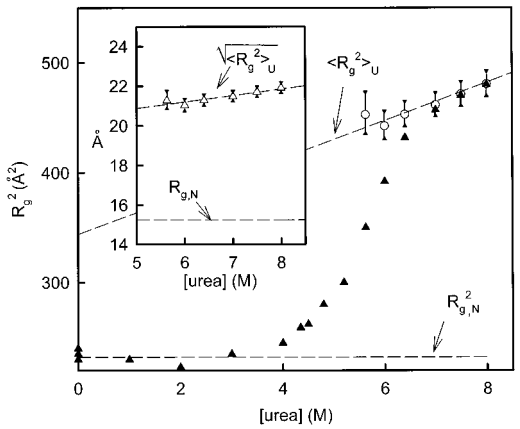

FIGURE 8: Deconvolution of the radius of gyration unfolding profile by using the values for the amount of native state derived from double-jump unfolding assays. (▲) Experimental values of the squared radius of gyration taken from Chen et al. (1996) and obtained at a protein concentration of 7 mg/mL. (○) Values for the average squared radius of gyration of the unfolded ensemble, obtained by using eq 12; the X_N values required for this calculation were calculated from the $m_{1/2}$ and $C_{1/2}$ values (Table 1) derived from the analysis of the double-jump unfolding assays carried out with a protein concentration in the initial solutions of 7 mg/mL; the $R_{g,N}^2$ value used was the average of the experimental values in the 0−3 M urea concentration range. The bars stand for the associated standard errors. The upper dashed line is the unfolded baseline obtained in the two-state global analysis shown in Figure 7; the excellent agreement of the calculated $\langle R_g^2 \rangle_U$ values with that unfolded baseline provides further support for the interpretation of the radius of gyration unfolding profile in terms of a two-state mechanism. The inset shows the calculated urea-concentration effect on the apparent radius of gyration of the unfolded state: $[\langle R_g^2 \rangle_U]^{1/2}$.

CONCLUDING REMARKS

This work points up some common pitfalls of the experimental detection of equilibrium folding intermediates. Thus, intermediate states are sometimes claimed to be significantly populated at equilibrium on the basis of comparatively small differences between experimental unfolding profiles obtained by using different physical probes. However, these may be apparent differences associated to baseline determination, rather than actual differences reflecting a non-two-state unfolding mechanism. In connection with this problem the following approaches may be useful:

(1) Global two-state analysis of the several unfolding profiles, imposing common values for the unfolding parameters, such as $m_{1/2}$ and $C_{1/2}$ (see Figure 7); a good global fit derived from such an analysis would obviously indicate that significant deviations from the two-state unfolding mechanism cannot be claimed on the basis of the analyzed unfolding profiles.

(2) Inclusion in the experimental profile analysis of the values of the measured physical property given by the zero-time extrapolations of the folding and unfolding kinetics; this procedure will minimize the uncertainties associated with baseline determination (see Figure 5), although it obviously assumes that the zero-time extrapolations yield the values corresponding to the native and unfolded states and not to burst intermediates in the time scales of the folding and refolding kinetic experiments.

(3) Use of experimental approaches that do not require baseline determination; for instance, double-jump unfolding assays [Figure 1; see also Figure 2 in Ibarra-Molero and Sanchez-Ruiz (1996)] and analysis of folding−unfolding kinetics (Chevron plots; see Figure 4A).

Also, small discrepancies between experimental unfolding profiles might conceivably be due to very small differences in some solvent condition, such as the pH value. Thus, energetic parameters for protein unfolding are often found to be strongly pH dependent [at least, within certain pH ranges; see, for instance Privalov (1979) and Pace et al. (1990, 1992)] and, under the normal laboratory practice, the pH cannot usually be measured and reproduced with a precission better than a few hundreths of a pH unit. In connection with this problem, the characterization of the unfolding process induced by changing the pH at denaturing concentrations of the denaturant used should be useful, since an estimate of the effect of pH irreproducibility may be easily derived from the sharpness of this pH-induced unfolding transition (see Figure 6).

Finally, recent work supports that equilibrium intermediate states in the thermal or solvent-induced unfolding of proteins may show a strong tendency to associate (Filimonov & Rogov, 1996; Semitsonov et al., 1996). Association will likely result in a significant protein concentration dependence of the equilibrium unfolding profiles, which suggests the convenience of having at our disposal experimental approaches that can be used in a wide protein concentration range. We note that, with an adequate design of the dilution steps, fluorescence-detected, double-jump unfolding and refolding assays (such as those employed in this work; Figures 1 and 3) may, in principle, be used with protein concentrations in the initial solutions as low as a few tenths of milligram per milliliter and as high as the solubility of the protein permits.

ACKNOWLEDGMENT

We thank Dr. V. V. Filimonov for stimulating discussions on protein folding intermediates.

REFERENCES

Alberty, R. A. (1969) *J. Am. Chem. Soc. 91*, 3899−3903.
Bates, R. G. (1973) *Determination of pH. Theory and Practice*, 2nd ed., Wiley, New York.
Brandts, J. F., Halvorson, H. R., & Brennan, M. (1975) *Biochemistry 14*, 4953−4963.
Canfield, R. E. (1963) *J. Biol. Chem. 238*, 2691−2697.
Chen, B.-L., Baase, W. A., Nicholson, H., & Schellman, J. A. (1992) *Biochemistry 31*, 1464−1476.
Chen, L., Hodgson, K. O., & Doniach, S. (1996) *J. Mol. Biol. 261*, 658−671
Denton, M. E., Rothwarf, D. M., & Scheraga, H. A. (1994) *Biochemistry 33*, 11225−11236.
Dobson, C. M. (1994) *Curr. Biol. 4*, 636−640.
Filimonov, V. V., & Rogov, V. V. (1996) *J. Mol. Biol. 255*, 767−777.
Fink, A. L. (1995) *Annu. Rev. Biophys. Biomol. Struct. 24*, 495−522.
Freire, E. (1995) *Annu. Rev. Biophys. Biomol. Struct. 24*, 141−165.
Griko, Y. V., Freire, E., Privalov, G., Dael, H. V., & Privalov P. L. (1995) *J. Mol. Biol. 252*, 447−459.
Haezebrouck, P., Joniau, M., Dael, H. V., Hooke, S. D., Woodruff, N. D., & Dobson, C. M. (1995) *J. Mol. Biol. 246*, 382−387.
Ibarra-Molero, B., & Sanchez-Ruiz, J. M. (1996) *Biochemistry 35*, 14689−14702.
Itzhaki, L. S., & Evans, P. A. (1996) *Protein Sci. 5*, 140−146.
Itzhaki, L. S., Evans, P. A., Dobson, C. M., & Radford, S. E. (1994) *Biochemistry 33*, 5212−5220.
Kato, S., Okamura, M., Shimamoto, N., & Utiyama, H. (1981) *Biochemistry 20*, 1080−1085.
Khechinashvili, N. N., Privalov, P. L., & Tiktopulo, E. I. (1973) *FEBS Lett. 30*, 57−60.
Kiefhaber, T. (1995) *Proc. Natl. Acad. Sci. U.S.A. 92*, 9029−9033.
Kim, P. S., & Baldwin, R. L. (1982) *Annu. Rev. Biochem. 51*, 459−489.
Kim, P. S., & Baldwin, R. L. (1990) *Annu. Rev. Biochem. 59*, 631−660.
Lu, H., Buck, M., Radford, S. E., & Dobson, C. M. (1997) *J. Mol. Biol. 265*, 112−117.
Makhatadze, G. I., & Privalov, P. L. (1992) *J. Mol. Biol. 226*, 491−505.
Mücke, M., & Schmid, F. X. (1994) *Biochemistry 33*, 12930−12935.
Pace, C. N., Shirley, B. A., & Thomson, J. A. (1989) in *Protein structure, a practical approach* (Creighton, T. E., Ed.) pp 311−330, IRL Press at Oxford University Press, Oxford.
Pace, C. N., Laurents, D. V., & Thomson, R. E. (1990) *Biochemistry 29*, 2564−2572.
Pace, C. N., Laurents, D. V., & Erickson, R. E. (1992) *Biochemistry 31*, 2728−2734.
Pfeil, W., & Privalov, P. L. (1976) *Biophys. Chem. 4*, 23−50.
Plaza del Pino, I. M., & Sanchez-Ruiz, J. M. (1995) *Biochemistry 34*, 8621−8630.
Privalov, P. L. (1979) *Adv. Protein Chem. 33*,167−241.
Privalov, P. L. (1996) *J. Mol. Biol. 258*, 707−725.
Privalov, P. L., & Khechinashvili, N. N. (1974) *J. Mol. Biol. 86*, *665*−684.
Ptitsyn, O. B. (1995) *Curr. Opin. Struct. Biol. 5*, 74−78.
Radford, S. E., Dobson, C. M., & Evans, P. A. (1992) *Nature 358*, 302−307.
Rothwarf, D. M., & Scheraga, H. A. (1996) *Biochemistry 35*, 13797−13087.
Schellman, J. A. (1987) *Annu. Rev. Biophys. Biophys. Chem. 16*, 115−137.
Schmid, F. X. (1992) in *Protein Folding* (Creighton, T. E., Ed.) pp 197−241, Freeman, New York.
Semitsonov, G. V., Kihara, H., Kotova, N. V., Kimura, K., Amemiya, Y., Wakabayashi, K., Serdyuk, I. N., Timchenko, A. A., Chiba, K., Nikaido, K., Ikura, T., & Kuwajima, K. (1996) *J. Mol. Biol. 262*, 559−574.
Smith, C. K., Bu, Z., Anderson, K. S., Sturtevant, J. M., Engelman, D. M., & Regan, L. (1996) *Protein Sci. 5*, 2009−2019.

BI9703305